Ab Initio Procedure for Aqueous-Phase pK_a Calculation: The Acidity of Nitrous Acid

Gabriel da Silva,[†] Eric M. Kennedy,* and Bogdan Z. Dlugogorski

Process Safety and Environment Protection Research Group, School of Engineering, The University of Newcastle, Callaghan, NSW 2308, Australia

Received: June 22, 2006; In Final Form: August 7, 2006

We present an ab initio procedure for accurately calculating aqueous-phase pK_a values and apply it to study the acidity of nitrous acid (HNO_2, or HONO). The aqueous-phase pK_a of nitrous acid was obtained from calculated gas-phase acidities and solvation free energies via a thermodynamic cycle and the solvation model chemistry of Barone et al. (*J. Chem. Phys.* **1997**, *107*, 3210). Solvation free energies were calculated at the HF/6-31G(d) level using the dielectric-polarizable continuum and the integral equation formalism-polarizable continuum solvent models (D-PCM and IEF-PCM, respectively), with the D-PCM model yielding the most accurate pK_a values. For HF free energies of solvation, significant improvements in accuracy could be made by moving to the larger 6-311++G(3df,3pd) and aug-cc-pVQZ basis sets. Solvation free energies were also calculated using the density functional theory (DFT) methods B3LYP, TPSS, PBE0, B1B95, VSXC, B98 and O3LYP, with the most accurate methods being TPSS and VSXC, which provided average errors of less than 0.11 pK_a units. Solvation free energies calculated with the different DFT methods were relatively insensitive to the basis set used. Our theoretical calculations are compared with experimental results obtained using stopped flow spectrophotometry. The pK_a of nitrous acid was measured as 3.16 at 25 °C, and the enthalpy and entropy of nitrous acid dissociation were calculated from measurements as 6.7 kJ mol^{-1} and −38.4 J mol^{-1} K^{-1}, respectively, between 25 and 45 °C. The UV/visible absorption spectra of the nitrite ion and nitrous acid were also examined, and molar extinction coefficients were obtained for each.

Introduction

The protonation of the nitrite ion to form nitrous acid is a reaction important to many fields of chemistry, and an accurate measurement of the pK_a value is therefore critical. Nitrous acid is found in the atmosphere[1] and has been implicated in the formation of NO_x and hydroxyl radicals.[2] Nitrous acid reacts with nucleophilic species to yield a range of nitrosating agents,[3] which can subsequently react with amines and amino acids to produce carcinogenic nitrosamines.[4] Nitrosation reactions are also of varied industrial significance.[5] The pK_a of nitrous acid has been determined numerous times, and measurements place it between 2.8 and 3.3,[2e,6] with the general consensus being that the correct value lies toward the upper limit of this range. There is less information on the temperature dependence of nitrous acid formation, with only two estimates of the enthalpy and entropy of reaction.[6a,b] One possible explanation for the wide range of pK_a values measured for nitrous acid is that nitrous acid spontaneously decomposes to NO_x under acidic conditions, albeit relatively slowly. Furthermore, in acidic solutions nitrite will be apportioned between the nitrite ion, nitrous acid and N_2O_3 (with very small amounts of ON^+), further complicating measurements.

Recent progress in computational chemistry has led to the development of composite theoretical techniques such as the complete basis set (CBS) and Gaussian-type (G*n*) methods, which have allowed researchers to accurately predict the thermodynamic properties of molecules of practical significance, including gas-phase pK_a values.[7] However, aqueous pK_a values are more difficult to calculate, due largely to errors associated with predicting solvation free energies. In this study we evaluate the accuracy with which a number of computational methods can predict both the gas- and aqueous-phase acidity of nitrous acid. A wide range of computational techniques, including ab initio, density functional theory and high-accuracy composite methods are employed. For the aqueous-phase calculations, several model chemistries for determining solvation free energies are evaluated. Calculated values for the aqueous-phase pK_a of nitrous acid are compared to an experimental measurement, which we obtain using stopped-flow spectrophotometry.

Experimental Section

Spectrophotometric measurements were made using a Pharmacia Ultrospec III UV/visible spectrophotometer. The reaction between nitrite and acid was conducted in an Applied Photophysics RX-2000 stopped flow cell, with a 10 mm path length. The stopped flow cell was temperature regulated to within ±0.05 °C using a Grant water bath. The reaction was initiated by mixing an equal volume of sodium nitrite solution with acidified water. The solution acidity was adjusted with sulfuric acid, and pH measurements were made by mixing equal volumes of the acid and nitrite solutions outside of the stopped-flow cell. De-ionized water was used in the preparation of all solutions. The use of a stopped-flow reaction cell, which is usually reserved for studying the kinetics of rapid chemical reactions, allows us to mix the reagents and perform spectrophotometric measurements over very small time scales, thus helping to minimize nitrite losses due to nitrous acid decomposition. Use of the stopped-flow apparatus also offers the advantage that the reagents are well temperature-regulated.

* To whom correspondence should be addressed. E-mail: eric.kennedy@newcastle.edu.au.

[†] Currently at Department of Chemistry and Environmental Science, New Jersey Institute of Technology, Newark, NJ 07102.

10.1021/jp0639243 CCC: $33.50
Published on Web 09/12/2006

SCHEME 1: Thermodynamic Cycle to Calculate the Aqueous-Phase Acidity of HNO_2

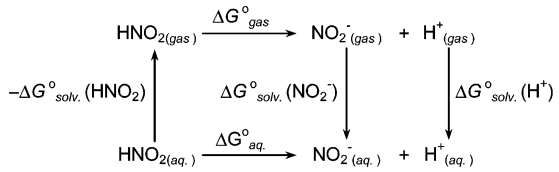

Theoretical Methods and Computational Details

Theoretical Calculation of pK_a. The accurate calculation of pK_a values using computational techniques is difficult, as there is no simple and precise way of theoretically evaluating the free energy of a solvated proton. Recent approaches, following the work of Liptak, Shields and co-workers,[8] have made use of the thermodynamic cycle depicted in Scheme 1.[9] Here, the gas-phase free energy of reaction is calculated using accurate theoretical techniques, and this value is then used with theoretical free energies of solvation to determine the aqueous free energy of reaction. Scheme 1 is formalized as eq 1.

$$\Delta G^\circ_{aq} = \Delta G^\circ_{gas} + \Delta G^\circ_{solv}(NO_2^-) + \Delta G^\circ_{solv}(H^+) - \Delta G^\circ_{solv}(HNO_2) \quad (1)$$

Equation 1 can be used to calculate $\Delta G^\circ_{aq.}$, and therefore pK_a, using theoretical values of ΔG°_{gas}, $\Delta G^\circ_{solv}(HNO_2)$, and $\Delta G^\circ_{solv}(NO_2^-)$, with an experimental value for $\Delta G^\circ_{solv}(H^+)$. The free energy of solvation of H^+ has recently been measured as -1104.5 kJ mol^{-1}.[10] A correction of $-RT$ ln V is also required in the calculations, to convert from a standard state of 1 atm to 1 M. Recent studies using similar thermodynamic cycles have resulted in pK_a predictions accurate to around 0.8−0.4 pK_a unit.[8,9]

Computational Details. All calculations were performed using Gaussian 03.[11] The gas-phase acidities of *cis*-HNO_2 and *trans*-HNO_2 were calculated using the Hartree−Fock (HF), MP2, QCISD(T) and B3LYP[12] methods. The 6-311++G(3df,-3pd) basis set was used with all theoretical methods, and the frozen core approximation was employed for the MP2 and QCISD(T) calculations, with the QCISD(T) calculations also featuring MP4 triples substitutions. For the QCISD(T) results, single point energy calculations were performed, using the B3LYP geometries and thermochemical corrections. In addition to these ab initio and DFT methods, the compound methods G1,[13] G2,[14] G2MP2,[15] G3,[16] G3MP2,[17] G3B3,[18] G3MP2B3,[18] CBS-4 (CBS-4M),[19,20] CBS-Q,[19] CBS-QB3[19,21] and CBS-APNO[19] were also used, giving a total of 15 theoretical methods. These 15 methods were used to calculate the gas-phase free energy of *cis*-HNO_2, *trans*-HNO_2 and NO_2^-. All predicted species had zero imaginary frequencies.

Free energies of solvation were calculated using the solvent model chemistry of Barone et al.,[22] who developed a set of optimized atomic radii for predicting accurate solvation free energies using the polarizable continuum model (PCM). The work of Barone et al.[22] used the Gaussian 94 implementation of the PCM, known as the dielectric polarizable continuum model (D-PCM).[23] To emulate these calculations in Gaussian 03, which has a dramatically different default PCM implementation, the solvent keyword DPCM was used,[24] with the setting ICOMP=4. The optimized atomic radii were invoked via the solvent keyword RADII=UAHF. Solvation free energies were then obtained using the SCFVAC keyword. In our simulations, we adopt the method of Barone et al.,[22] in which solvation free energies were determined at the HF level of theory, with the 6-31G(d) basis set for neutral molecules and the 6-31+G(d) basis set for anions. Calculations were performed on gas-phase geometries, which were obtained using each of the 15 different theoretical methods (for the compound theoretical techniques involving two levels of geometry optimization, such as CBS-Q and G3, the highest-level geometry is used). Variations on the model chemistry of Barone et al.[22] were also examined, where calculations were performed using a number of larger basis sets, as well as using different DFT methods. The basis sets tested are 6-311++G(3df,3pd) and the double-, triple- and quadruple-ζ correlation consistent basis sets aug-cc-pVDZ, aug-cc-pVTZ and aug-cc-pVQZ. The DFT methods tested are B3LYP,[12] TPSS,[25] PBE0,[26] B1B95,[12a,27] VSXC,[28] B98,[29] and O3LYP.[12b,30] Furthermore, a second solvent model chemistry was tested, which featured the default Gaussian 03 PCM implementation, the integral equation formalism-polarizable continuum model (IEF-PCM).[31] All other computational settings were kept the same as in the above solvent calculations, though the redundant ICOMP keyword was not used.

It should be noted that continuum solvent models of the type used in this study do not account for individual hydrogen bonds that may form between solvent and solute molecules. For those instances where hydrogen bonding is important, discrete solvent methods may be better suited, where solvent cages consisting of discrete solvent molecules are constructed around the solute molecule. These methods have the advantage of implicitly describing solvent−solute interactions, although the addition of discrete solvent molecules means that calculations need to be performed on relatively large molecular complexes, whereas the construction of realistic solvent cages can be difficult and time-consuming. A further class of solvent model chemistries, which employ a hybrid discrete-continuum approach, solve some of the problems encountered with the discrete approach to solvation. Here, a small number of solvent molecules are bound to the solute molecule, with the entire solvent−solute complex then placed within a continuum solvent field. We do not expect either nitrous acid or the nitrite ion to undergo significant hydrogen bonding, justifying our choice of continuum solvent models, although it is important to consider the possible presence of solvent−solute hydrogen bonding when applying the techniques described in this study to other molecules.

Results and Discussion

Experimental Measurement of pK_a. *Nitrite Ion Spectra.* According to Beer's law, the following relationship can be demonstrated between absorbance (A), total nitrite concentration $[NO_2^-]_T$, and molar extinction coefficient (ϵ).

$$A = \epsilon[NO_2^-]_T \quad (2)$$

Here, the total nitrite concentration includes the species NO_2^-, HNO_2, and N_2O_3. The molar extinction coefficient, with units of M^{-1} cm^{-1}, takes into account the 1 cm path length of the spectrophotometer cell. The following relationship denotes the absorbance of a nitrite solution as a function of the concentrations and extinction coefficients of the discrete nitrite components.

$$A = \epsilon_{NO_2^-}[NO_2^-] + \epsilon_{HNO_2}[HNO_2] + \epsilon_{N_2O_3}[N_2O_3] \quad (3)$$

At low acidity, the only nitrite species present in appreciable quantities are the nitrite ion and nitrous acid, thus allowing the following simplification:

$$A = \epsilon_{NO_2^-}[NO_2^-] + \epsilon_{HNO_2}[HNO_2] \quad (4)$$

At even lower acid concentrations, the nitrite ion becomes the only significant species in solution, and the extinction coefficient of the nitrite ion can therefore be readily determined.

To measure the nitrite ion spectrum, standard sodium nitrite solutions were prepared at neutral pH and then mixed in the stopped-flow reaction cell. Figure 1 shows the absorption spectra obtained from these experiments at wavelengths of 240−440 nm. No significant absorption was detected in any of the experimental runs above 440 nm. From Figure 1 it can be seen that the nitrite ion demonstrates a strong absorbance peak at 352 nm, with a lesser band of absorption between 265 and 310 nm. According to Beer's law, nitrite ion extinction coefficients were calculated at each wavelength from 240 to 440 nm for each of the experimental runs shown in Figure 1. The average results are presented in Figure 2. The molar extinction coefficient at the peak wavelength of 352 nm is 21.8 ± 0.5 M^{-1} cm^{-1}, where the uncertainty is taken to be the standard deviation of the extinction coefficients measured at each of the different nitrite ion concentrations.

pK_a Measurement. The value of K_a has been determined using the technique of Ho,[6a] where K_a is obtained from a series of measurements in solutions of varying acidity. From eq 5, which is derived by Ho,[6a] we find that a plot of $(\epsilon - \epsilon_{NO_2^-})/[H^+]$ vs ϵ provides a linear relationship with slope of K_a and intercept of ϵ_{HNO_2}.

$$\epsilon = \epsilon_{HNO_2} - \frac{K_a(\epsilon - \epsilon_{NO_2^-})}{[H^+]} \quad (5)$$

The equilibrium constant for nitrous acid dissociation was determined at the four peak wavelengths of nitrous acid, for measurements in the pH range 1.6−3.0 at 25 °C. Separate experiments on the nitrous acid spectra identified these peaks at 346, 357, 369, and 383 nm. The nitrous acid absorption spectrum is presented in the Supporting Information.

Figure 3 shows the plot of $(\epsilon - \epsilon_{NO_2^-})/[H^+]$ vs ϵ, and we find good linearity across all results for the four wavelengths. From the average slope of the four plots, we evaluate K_a to be 6.93×10^{-4} M, or a pK_a value of 3.16. From the intercepts at each of the wavelengths we can also calculate ϵ_{HNO_2} values. We find extinction coefficients of 36.9, 47.8, 50.4, and 30.3 M^{-1} cm^{-1} at wavelengths of 346, 357, 369, and 383 nm, respectively. Comparatively, Markovits et al.[32] measured peak extinction coefficients of 32.8, 47.7, 49.4, and 28.6 M^{-1} cm^{-1} at wavelengths of 347, 358, 371, and 386 nm, respectively, showing relatively good agreement with our results.

To determine the effect of temperature on the deprotonation of nitrous acid, pK_a measurements were made at 45 °C. Calculations followed the same procedure as for the measurement at 25 °C, except absorbance readings were only made at 357 and 369 nm, and for fewer pH values. From the plot of $(\epsilon - \epsilon_{NO_2^-})/[H^+]$ vs ϵ shown in Figure 4, the pK_a of nitrous acid at 45 °C is found to be 3.08 ($K_a = 8.20 \times 10^{-4}$ M). Comparing the 25 and 45 °C results, we discover that the enthalpy of dissociation is 6.7 kJ mol^{-1} and the entropy of dissociation is −38.4 J mol^{-1} K^{-1}. These values compare well with previous enthalpy measurements of 9.2 and 6.2 kJ mol^{-1} and entropy measurements of −30 and −37 J mol^{-1} K^{-1}.[6a,b]

Theoretical Calculation of pK_a. *Gas-Phase Acidity of Nitrous Acid.* Gas-phase acidities were calculated for *cis*- and *trans*-HNO_2 using the 15 computational methods described above. The resultant acidities are reported in Table 1, along with the average acidity for the two conformations. A linear average was used, as the two conformers are very close in energy; all 15 methods predict *cis*- and *trans*-HNO_2 to be within around 4 kJ mol^{-1} of each other. Table 1 also includes the error between the predicted acidities and the experimentally measured value of 1396.2 kJ mol^{-1}.[33] From Table 1 we find that the HF, G1, MP2 and B3LYP methods show the largest discrepancies

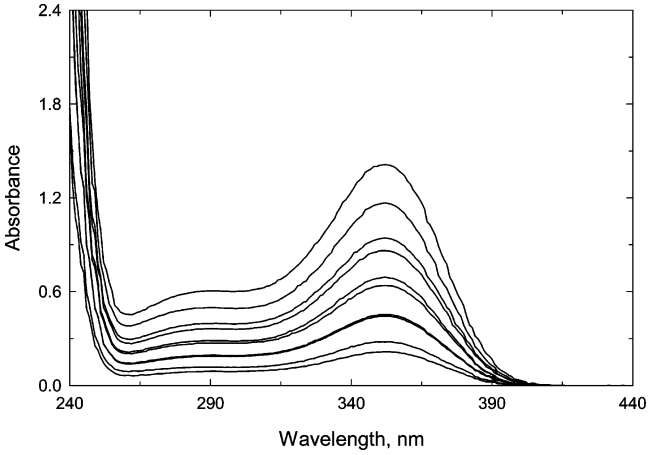

Figure 1. Aqueous absorption spectrum of the nitrite ion, from concentrations of 0.01017 to 0.06455 M.

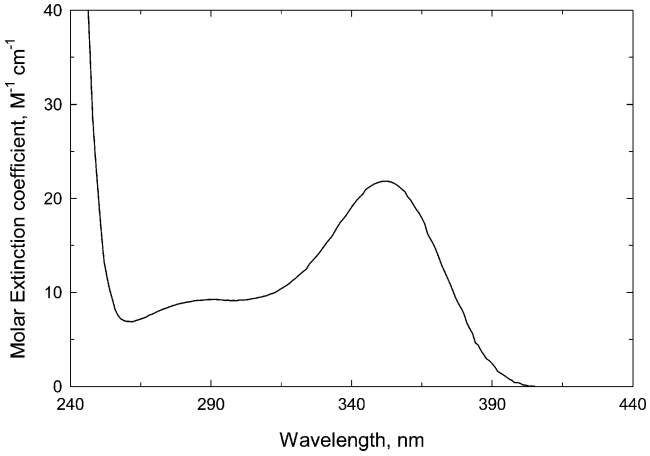

Figure 2. Molar extinction coefficients for the nitrite ion between 240 and 440 nm.

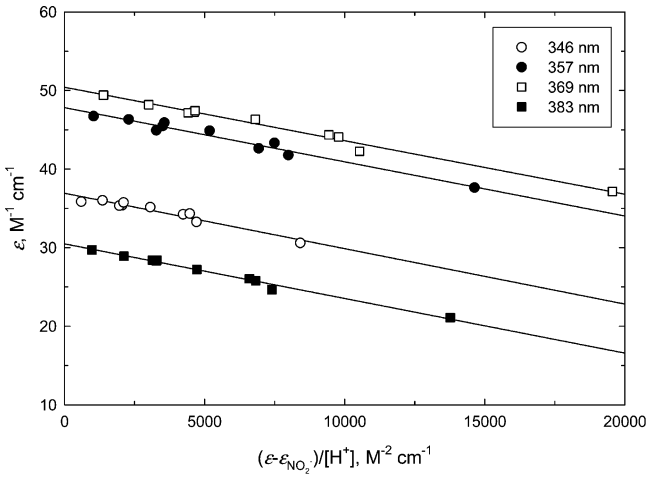

Figure 3. Absorbance of 0.05 M nitrous acid solutions in the pH range 1.6−3.0, at 25 °C for wavelengths 346, 357, 369, and 383 nm.

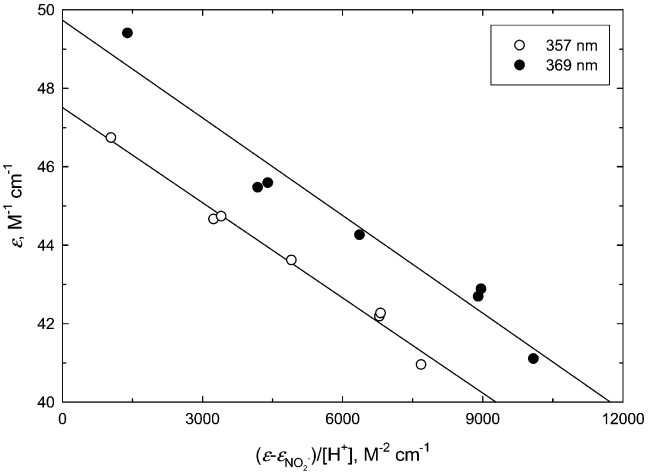

Figure 4. Absorbance of 0.05 M nitrous acid solutions in the pH range 1.6−2.6, at 45 °C for wavelengths 357 and 369 nm.

TABLE 1: Gas-Phase Free Energy ($\Delta G°_{gas}$, kJ mol^{-1}) of Deprotonation for *cis*-HNO_2 and *trans*-HNO_2 and Error of the Average Value Relative to the Experimental Measurement

	cis-HNO_2	*trans*-HNO_2	HNO_2 (av)	error
HF	1416.1	1415.3	1415.7	19.5
MP2	1383.8	1385.8	1384.8	−11.4
QCISD(T)	1400.1	1401.9	1401.0	4.8
B3LYP	1386.2	1388.5	1387.4	−8.8
G1	1382.3	1385.6	1383.9	−12.3
G2	1388.2	1390.8	1389.5	−6.7
G2MP2	1393.1	1395.4	1394.3	−1.9
G3	1390.5	1393.2	1391.8	−4.4
G3MP2	1394.7	1397.6	1396.2	0.0
G3B3	1392.5	1395.3	1393.9	−2.3
G3MP2B3	1396.6	1399.7	1398.1	1.9
CBS-4	1387.4	1392.1	1389.8	−6.4
CBS-Q	1389.8	1392.1	1390.9	−5.3
CBS-QB3	1389.4	1391.3	1390.4	−5.8
CBS-APNO	1391.3	1393.4	1392.4	−3.8

compared with the experimental value, with errors of over 8 kJ mol^{-1}. These results highlight the importance of electron correlation, which is not thoroughly accounted for in any of these methods. The remaining computational techniques all adequately predict the experimental acidity, with errors of less than 7 kJ mol^{-1}.

Aqueous-Phase pK_a. Free energies of solvation were calculated for NO_2^-, *cis*-HNO_2 and *trans*-HNO_2, according to the procedure described above, with both the D-PCM and IEF-PCM solvent models. Consistent with the method of Barone et al.,[22] the gas-phase geometries obtained with each of the 14 computational methods were used, as the relaxation energy upon solvation is typically small. The free energies of solvation are provided as Supporting Information. Table 2 lists the conformationally averaged pK_a values obtained using each of the solvation models with all 14 gas-phase acidities, along with the error of the predicted values, relative to our experimental measurement of 3.16.

Table 2 illustrates that, in all instances, the pK_a values predicted using the D-PCM model are more accurate than those obtained using the IEF-PCM model. With the D-PCM model, the best predictions are typically provided by the high-level composite methods, such as CBS-APNO, CBS-QB3 and G2. Overall, the smallest error is obtained with the B3LYP method, although this is most likely due to error cancellation between the gas-phase pK_a and the aqueous solvation free energies, as discussed below. The superiority of the Gaussian 98 D-PCM model over the Gaussian 03 IEF-PCM model is interesting, considering the significant advances embodied in the 03 PCM model. We believe that the success of the D-PCM model stems from the fact that the atomic radii used in our calculations are optimized for this model, and not the Gaussian 03 PCM model. Accordingly, there could be much usefulness in a set of atomic radii optimized for the current PCM solvent model. Determining a new set of atomic radii for the IEF-PCM model is, however, outside the scope of this study, in which we are only examining the pK_a of one molecule.

TABLE 2: Calculated pK_a Values and Relative Errors for the D-PCM and IEF-PCM Solvent Models

	D-PCM		IEF−PCM	
	pK_a	error	pK_a	error
HF	7.37	4.21	9.23	6.07
MP2	2.61	−0.55	4.21	1.05
QCISD(T)	5.24	2.08	6.93	3.77
B3LYP	2.86	−0.30	4.54	1.38
G1	2.54	−0.62	4.41	1.25
G2	3.93	0.77	5.38	2.22
G2MP2	4.34	1.18	6.21	3.05
G3	4.33	1.17	5.81	2.65
G3MP2	5.08	1.92	6.57	3.41
G3B3	4.42	1.26	5.97	2.81
G3MP2B3	5.17	2.01	6.71	3.55
CBS-4	3.68	0.52	5.21	2.05
CBS-Q	3.99	0.83	5.51	2.35
CBS-QB3	3.58	0.42	5.13	1.97
CBS-APNO	3.89	0.73	5.50	2.34

A note about the B3LYP density functional results: With the D-PCM model, the B3LYP functional returns the pK_a value in closest agreement with our own experimental value. However, when one considers the relatively large error observed for the gas-phase acidity of nitrous acid calculated at the B3LYP level (ca. 8 kJ mol^{-1}), the success of the B3LYP functional at predicting the aqueous pK_a of nitrous acid may in part be due to a fortuitous cancellation of errors. Furthermore, the B3LYP functional is known to be especially poor at describing long-range and nonbonded interactions, which are not present in nitrous acid or the nitrite ion. For instance, we recently demonstrated that B3LYP calculations using double-, triple- and quadruple-ζ correlation consistent basis sets, extrapolated to the complete basis set limit, systematically overpredicted the heterolytic bond energy of several aqueous nitroso compounds by more than 30 kJ mol^{-1}.[34] Although the computational efficiency and generally good accuracy of the B3LYP method may make it attractive to study the aqueous pK_a of large organic and/or biologically active molecules, it is important to keep the above caveats in mind.

We have investigated three variations on the D-PCM solvent model of Barone et al.[22] First, solvation free energies were calculated using the larger 6-311++G(3df,3pd), aug-cc-pVDZ, aug-ccpVTZ, and aug-cc-pVQZ basis sets. Second, solvation free energies were calculated with a variety of DFT methods, using each of the different basis sets. Calculated pK_a values are reported here only for the accurate G2, CBS-Q, CBS-QB3, and CBS-APNO theoretical methods. The HF results are presented in Table 3, and the DFT results are given in Table 4.

From Table 3 we observe that, with the HF method, increasing the size of the basis set offers a significant increase in accuracy (excluding the aug-cc-pVTZ basis set) over the 6-31G(d) results; with solvation free energies calculated at the HF/aug-cc-pVQZ level of theory, the average error is less than 0.4 pK_a units, whereas the HF/6-31G(d) calculations result in an average error of almost 0.7 pK_a units. Table 4 reveals,

TABLE 3: Nitrous Acid pK_a Values Calculated Using HF Solvation Free Energies Calculated with Different Basis Sets in the D-PCM Solvent Model Chemistry, with Gas-Phase pK_a Values and Geometries from Four Composite Theoretical Methods

	HF/6-31G(d)[a]	HF/6-311++G(3df,3pd)	HF/aug-cc-pVDZ	HF/aug-cc-pVTZ	HF/aug-cc-pVQZ
G2	3.93	3.79	3.77	3.83	3.59
CBS-Q	3.99	3.84	3.82	3.87	3.68
CBS-QB3	3.58	3.42	3.39	3.45	3.29
CBS-APNO	3.89	3.72	3.70	3.75	3.64
error[b]	0.69	0.53	0.51	0.57	0.39

[a] 6-31+G(d) for the NO_2^- ion. [b] Absolute average error, relative to the experimental value of 3.16.

TABLE 4: Nitrous Acid pK_a Values Calculated Using Free Energies Calculated with Different Basis Sets and DFT Methods in the D-PCM Solvent Model Chemistry[a]

	6-31G(d)[b]	6-311++G(3df,3pd)	aug-cc-pVDZ	aug-cc-pVTZ	aug-cc-pVQZ	error[c]
B3LYP	3.42	3.40	3.42	3.52	3.53	0.30
TPSS	3.13	3.02	3.08	3.18	3.45	0.11
PBE0	3.32	3.23	3.24	3.32	3.61	0.18
B1B95	3.32	3.25	3.21	3.32	3.40	0.14
VSXC	3.14	3.10	3.23	3.29	3.28	0.08
B98	3.33	3.24	3.23	3.37	3.22	0.12
O3LYP	3.24	2.73	3.36	3.45	3.64	0.30

[a] Average pK_a values calculated using G2, CBS-Q, CBS-QB3 and CBS-APNO gas-phase pK_a values and geometries. [b] 6-31+G(d) for the NO_2^- ion. [c] Absolute average error, relative to the experimental value of 3.16.

however, that a more dramatic improvement is made with the DFT methods. Each of the DFT methods reproduces the pK_a of nitrous acid to within around 0.3 pK_a units, on average. The most successful methods are VSXC, TPSS, B98, and B1B95, which all provide average errors of less than 0.15 pK_a units; this average error of 0.15 pK_a units is less than half that reported in many accurate ab initio pK_a studies,[8,9] highlighting the accuracy of the proposed methodology. Furthermore, almost all of the pK_a values calculated using the different DFT methods fall within the range of experimentally measured values, and the average discrepancy between the experimental pK_a and the average DFT values is probably within the experimental error of our pK_a measurement. In general, the pK_a values calculated using the DFT methods are greater than the experimental measurement, being around 3.3 on average, although it is unclear whether this discrepancy can be attributed to experimental error, or computational errors in the gas-phase pK_a values and/or in the free energies of solvation. It is also interesting to note that the DFT results show no discernible benefit in using the larger basis sets. Similar results were observed by Takano and Houk,[35] in their study of aqueous solvation free energies with different PCM solvent models. Here, smaller 6-31G-type basis sets were found to provide the most accurate solvation free energies with both HF and DFT methods.

The above calculations made use of gas-phase geometries to predict solvation free energies. In reality, the molecular geometry will undergo relaxation upon solvation, and an aqueous-phase geometry should therefore be used for the liquid-phase component of solvation free energy calculations. The effect of geometry relaxation has been studied for the accurate CBS-QB3 and CBS-APNO methods, with the D-PCM B3LYP/6-311++G(3df,3pd) solvent model. Table 5 compares the solvation free energies and average pK_a values calculated using the gas- and aqueous-phase geometries. We find that the pK_a predictions are deleteriously affected by using the aqueous-phase geometries. As with the IEF-PCM results, we believe that this error arises from using atomic radii optimized under different conditions, in this case, using gas-phase geometries. For the estimation of high-accuracy solvation free energies, atomic radii optimized for aqueous-phase geometries may be necessary.

TABLE 5: Predicted Solvation Free Energies (ΔG°_{solv}, kJ mol^{-1}) and pK_a Values for Gas- and Aqueous-Phase Geometries[a]

	trans-HNO_2	*cis*-HNO_2	NO_2^-	pK_a
		Gas-Phase Geometry		
CBS-QB3	−5.07	−4.70	−67.01	3.16
CBS-APNO	−5.34	−4.55	−67.08	3.50
		Aqueous-Phase Geometry		
CBS-QB3	−6.18	−5.42	−67.06	3.77
CBS-APNO	−6.09	−5.15	−67.14	3.94

[a] Solvation free energies are calculated with the D-PCM B3LYP/6-311++G(3df,3pd) solvent model.

Conclusion

The acidity of nitrous acid has been investigated using both experimental and computational techniques. Stopped-flow spectrophotometry was used to determine the UV/visible absorption spectra of the nitrite ion and nitrous acid. The pK_a of nitrous acid was measured as 3.16 at 25 °C. Between 25 and 45 °C, the enthalpy and entropy of nitrous acid dissociation were measured as 6.7 kJ mol^{-1} and −38.4 J mol^{-1} K^{-1}, respectively.

The aqueous-phase pK_a of nitrous acid was predicted via a thermodynamic cycle, utilizing calculated gas-phase acidities and solvation free energies. The gas-phase acidity of nitrous acid was calculated using 15 theoretical methods, of which the high-level composite techniques were generally the most accurate. Solvation free energies were predicted using the model chemistry of Barone et al.,[22] with both the D-PCM and IEF-PCM solvent models. The pK_a values calculated using the D-PCM model, for all 15 theoretical methods, were more accurate than those obtained using the IEF-PCM model. This was attributed to the use of atomic radii optimized for the D-PCM model. Solvation free energies were calculated using a series of larger basis sets, and significant improvements were made using the 6-311+G(3df,3pd) and aug-cc-pVQZ basis sets. Solvation free energies were also calculated using a selection of DFT methods, which saw large improvements over similar HF results. The most successful DFT methods were TPSS and VSXC, which reproduced the pK_a of nitrous acid to within an average error of 0.2 pK_a units.

Acknowledgment. This work was supported by funding from the Australian Research Council (ARC) and Orica Explosives.

Supporting Information Available: Absorption spectra of nitrous acid. Cartesian coordinates, energies and free energies for all optimized geometries. Calculated solvation free energies. This material is available free of charge via the Internet at http://pubs.acs.org.

References and Notes

(1) (a) Kleffmann, J.; Gavriloaiei, T. *Geophys. Res. Lett.* **2005**, *32*, L05818. (b) Park, S. S.; Hong. S. B.; Jung, Y. G.; Lee, J. H. *Atmos. Environ.* **2004**, *38*, 293.

(2) (a) Alicke, B.; Geyer, A.; Hofzumahaus, A.; Holland, F.; Konrad, S.; Pätz, H. W.; Schäfer, J.; Stutz, J.; Volz-Thomas, A.; Platt, U. *J. Geophys. Res.* **2003**, *108*, 8247. (b) Stemmler, K.; Ammann, M.; Donders, C.; Kleffmann, J.; George, C. *Nature* **2006**, *440*, 195. (c) Lammel, G.; Cape, J. N. *Chem. Soc. Rev.* **1996**, 361. (d) Platt, U.; Perner, D.; Harris, G. W.; Winer, A. M.; Pitts, J. N. *Nature* **1980**, *285*, 312. (e) Riordan, E.; Minogue, N.; Healy, D.; O'Driscoll, P.; Sodeau, J. R. *J. Phys. Chem. A* **2005**, *109*, 779.

(3) da Silva, G.; Kennedy, E. M.; Dlugogorski, B. Z. *J. Chem. Res. (S)* **2002**, 589.

(4) (a) da Silva, G.; Kennedy, E. M.; Dlugogorski, B. Z. *J. Phys. Org. Chem.*, in press. (b) da Silva, G.; Kennedy, E. M.; Dlugogorski, B. Z. *J. Am. Chem. Soc.* **2005**, *127*, 3664. (c) da Silva, G.; Kennedy, E. M.; Dlugogorski, B. Z. *Ind. Eng. Chem. Res.* **2004**, *43*, 2296.

(5) (a) da Silva, G.; Dlugogorski, B. Z.; Kennedy, E. M. *Chem. Eng. Sci.* **2006**, *61*, 3186. (b) da Silva, G.; Dlugogorski, B. Z.; Kennedy, E. M. *AIChE J.* **2006**, *52*, 1558. (c) Nguyen, D. A.; Faria de Moraes, F.; Fogler, H. S. *Ind. Eng. Chem. Res.* **2004**, *43*, 5862. (d) Nguyen, D. A.; Iwaniw, M. A.; Fogler, H. S. *Chem. Eng. Sci.* **2003**, *58*, 4351.

(6) (a) Ho, W. H. *Proc. Nat. Sci. Counc.* **1977**, *10*, 175. (b) Lumme, P.; Tummavuori, J. *Acta Chem. Scand.* **1965**, *19*, 617. (c) Park, J.; Lee, Y. *J. Phys. Chem.* **1988**, *92*, 6294. (d) Vassian, E. G.; Eberhardt, W. H. *J. Phys. Chem.* **1958**, *62*, 84.

(7) (a) Alexeev, Y.; Windus, T. L.; Zhan, C.-G.; Dixon, D. A. *Int. J. Quantum Chem.* **2005**, *102*, 775. (b) Tossell, J. A. *Geochim. Cosmochim. Acta* **2005**, *69*, 5647.

(8) (a) Liptak, M. D.; Gross, K. C.; Seybold, P. G.; Feldgus, S.; Shields, G. C. *J. Am. Chem. Soc.* **2002**, *124*, 6421. (b) Liptak, M. D.; Shields, G. C. *Int. J. Quantum Chem.* **2001**, *85*, 727. (c) Liptak, M. D.; Shields, G. C. *J. Am. Chem. Soc.* **2001**, *123*, 7314.

(9) (a) Cao, Z.; Lin, M.; Zhang, Q.; Mo, Y. *J. Phys. Chem. A* **2004**, *108*, 4277. (b) da Silva, C. O.; da Silva, E. C.; Nascimento, M. A. C. *J. Phys. Chem. A* **1999**, *103*, 11194. (c) Gao, D.; Svoronos, P.; Wong, P. K.; Maddalena, D.; Hwang, J.; Walker, H. *J. Phys. Chem. A* **2005**, *109*, 10776. (d) Magill, A. M.; Cavell, K. J.; Yates, B. F. *J. Am. Chem. Soc.* **2004**, *126*, 8717. (e) Magill, A. M.; Yates, B. F. *Aust. J. Chem.* **2004**, *57*, 1205. (f) Murlowska, K.; Sadlej-Sosnowska, N. *J. Phys. Chem. A* **2005**, *109*, 5590. (g) M Namazian, M.; Heidary, H. *J. Mol. Struct. (THEOCHEM)* **2003**, *620*, 257. (h) Namazian, M.; Kalantary-Fotooh, F.; Noorbala, M. R.; Searles, D. J.; Coote, M. L. *J. Mol. Struct. (THEOCHEM)* **2005**, *758*, 273. (i) Saracino, G. A. A.; Improta, R.; Barone, V. *Chem. Phys. Lett.* **2003**, *373*, 411.

(10) Tissandier, M. D.; Cowen, K. A.; Feng, W. Y.; Gundlach, E.; Cohen, M. H.; Earhart, A. D.; Coe, J. V.; Tuttle, T. R. *J. Phys. Chem. A* **1998**, *102*, 7787.

(11) Frisch, M. J.; Trucks, G. W.; Schlegel, H. B.; Scuseria, G. E.; Robb, M. A.; Cheeseman, J. R.; Montgomery, J. A., Jr.; Vreven, T.; Kudin, K. N.; Burant, J. C.; Millam, J. M.; Iyengar, S. S.; Tomasi, J.; Barone, V.; Mennucci, B.; Cossi, M.; Scalmani, G.; Rega, N.; Petersson, G. A.; Nakatsuji, H.; Hada, M.; Ehara, M.; Toyota, K.; Fukuda, R.; Hasegawa, J.; Ishida, M.; Nakajima, T.; Honda, Y.; Kitao, O.; Nakai, H.; Klene, M.; Li, X.; Knox, J. E.; Hratchian, H. P.; Cross, J. B.; Adamo, C.; Jaramillo, J.; Gomperts, R.; Stratmann, R. E.; Yazyev, O.; Austin, A. J.; Cammi, R.; Pomelli, C.; Ochterski, J. W.; Ayala, P. Y.; Morokuma, K.; Voth, G. A.; Salvador, P.; Dannenberg, J. J.; Zakrzewski, V. G.; Dapprich, S.; Daniels, A. D.; Strain, M. C.; Farkas, O.; Malick, D. K.; Rabuck, A. D.; Raghavachari, K.; Foresman, J. B.; Ortiz, J. V.; Cui, Q.; Baboul, A. G.; Clifford, S.; Cioslowski, J.; Stefanov, B. B.; Liu, G.; Liashenko, A.; Piskorz, P.; Komaromi, I.; Martin, R. L.; Fox, D. J.; Keith, T.; Al-Laham, M. A.; Peng, C. Y.; Nanayakkara, A.; Challacombe, M.; Gill, P. M. W.; Johnson, B.; Chen, W.; Wong, M. W.; Gonzalez, C.; Pople, J. A. *Gaussian 03*, revision B.05; Gaussian, Inc.: Pittsburgh, PA, 2003.

(12) (a) Becke, A. D. *Phys. Rev. A* **1988**, *38*, 3098. (b) Lee, C.; Yang, W.; Parr, R. G. *Phys. Rev. B* **1988**, *37*, 785.

(13) Pople, J. A.; Head-Gordon, M.; Fox, D. J.; Raghavachari, K.; Curtiss, L. A. *J. Chem. Phys.* **1989**, *90*, 5622.

(14) Curtiss, L. A.; Raghavachari, K.; Trucks, G. W.; Pople, J. A. *J. Chem. Phys.* **1991**, *94*, 7221.

(15) Curtiss, L. A.; Raghavachari, K.; Pople, J. A. *J. Chem. Phys.* **1993**, *98*, 1293.

(16) Curtiss, L. A.; Raghavachari, K.; Redfern, P. C.; Rassolov, V.; Pople, J. A. *J. Chem. Phys.* **1998**, *109*, 7764.

(17) Curtiss, L. A.; Redfern, P. C.; Raghavachari, K.; Rassolov, V.; Pople, J. A. *Chem. Phys.* **1999**, *110*, 4703.

(18) Baboul, A. G.; Curtiss, L. A.; Redfern, P. C.; Raghavachari, K. *J. Chem. Phys.* **1999**, *110*, 7650.

(19) Ochterski, J. W.; Petersson, G. A.; Montgomery, J. A. *J. Chem. Phys.* **1996**, *104*, 2598.

(20) Montgomery, J. A.; Frisch, M. J.; Ochterski, J. W.; Petersson, G. A. *J. Chem. Phys.* **2000**, *112*, 6532.

(21) Montgomery, J. A.; Frisch, M. J.; Ochterski, J. W.; Petersson, G. A. *J. Chem. Phys.* **1999**, *110*, 2822.

(22) Barone, V.; Cossi, M.; Tomasi, J. *J. Chem. Phys.* **1997**, *107*, 3210.

(23) (a) Cossi, M.; Barone, V.; Cammi, R.; Tomasi, J. *Chem. Phys. Lett.* **1996**, *255*, 327. (b) Miertus, S.; Scrocco, E.; Tomasi, J. *Chem. Phys.* **1981**, *55*, 117. (c) Miertus, S.; Tomasi, J. *Chem. Phys.* **1982**, *65*, 239.

(24) Cossi, M.; Scalmani, G.; Rega, N.; Barone, V. *J. Chem. Phys.* **2002**, *117*, 43.

(25) Tao, J.; Perdew, J. P.; Staroverov, V. N.; Scuseria, G. E. *Phys. Rev. Lett.* **2003**, *91*, 146401.

(26) Adamo, C.; Barone, V. *J. Chem. Phys.* **1999**, *110*, 6158.

(27) Becke, A. D. *J. Chem. Phys.* **1996**, *104*, 1040.

(28) Van Voorhis, T.; Scuseria, G. E. *J. Chem. Phys.* **1998**, *109*, 400.

(29) Schmider, H. L.; Becke, A. D. *J. Chem. Phys.* **1998**, *108*, 9624.

(30) (a) Handy, N. C.; Cohen, A. J. *Mol. Phys.* **2001**, *99*, 403. (b) Handy, N. C.; Cohen, A. J. *Mol. Phys.* **2001**, *99*, 607.

(31) (a) Cancès, E.; Mennucci, B.; Tomasi, J. *J. Chem. Phys.* **1997**, *107*, 3032. (b) Mennucci, B.; Cancès, E.; Tomasi, J. *J. Phys. Chem. B* **1997**, *101*, 10506. (c) Mennucci, B.; Tomasi, J. *J. Chem. Phys.* **1997**, *106*, 5151. (d) Tomasi, J.; Mennucci, B.; Cancès, E. *J. Mol. Struct.* (THEOCHEM) **1999**, *464*, 211.

(32) Markovits, G. Y.; Schwartz, S. E.; Newman, L. *Inorg. Chem.* **1981**, *20*, 445.

(33) Ervin, K. M.; Ho, J.; Lineberger, W. C. *J. Phys. Chem.* **1988**, *92*, 5405.

(34) da Silva, G.; Kennedy, E. M.; Dlugogorski, B. Z. *J. Phys. Chem. A* **2006**, *submitted*.

(35) Takano, Y.; Houk, K. N. *J. Chem. Theory Comput.* **2005**, *1*, 70.